

# Spontaneous Fermi surface deformation in the three-band Hubbard model: A variational Monte Carlo study

Xiao-Jun Zheng,<sup>1</sup> Zhong-Bing Huang,<sup>2,3,\*</sup> and Liang-Jian Zou<sup>1,†</sup>

<sup>1</sup>Key Laboratory of Materials Physics, Institute of Solid State Physics,  
Chinese Academy of Sciences, P. O. Box 1129, Hefei 230031, China

<sup>2</sup>Faculty of Physics and Electronic Technology, Hubei University, Wuhan 430062, China

<sup>3</sup>Beijing Computational Science Research Center, Beijing 100084, China

(Dated: December 11, 2013)

We perform a variational Monte Carlo study on spontaneous  $d$ -wave form Fermi surface deformation ( $d$ FSD) within the three-band Hubbard model. It is found that the variational energy of a projected Fermi sea is lowered by introducing an anisotropy between the hopping integrals along the  $x$  and  $y$  directions. Our results show that the  $d$ FSD state has the strongest tendency at half-filling in the absence of magnetism, and disappears as the hole concentration increases to  $n_h \approx 1.15$ . This is qualitatively in agreement with the mean field analysis and the exact diagonalization calculation for the one-band models, and provides a qualitative explanation to the “intra-unit-cell” electronic nematicity revealed by the scanning tunneling microscopy. An analysis of the dependence of  $d$ FSD on the parameters of the three-band model indicates that the copper on-site Coulomb interaction, the nearest-neighbor copper-oxygen repulsion, and the charge-transfer energy have a remarkable positive effect on  $d$ FSD.

PACS number(s): 74.20.Mn, 71.10.Li, 71.10.Fd

## I. INTRODUCTION

High temperature superconductivity is realized by doping charge carriers into an antiferromagnetic insulator. In the underdoped region which lies between half-filling and optimal doping, competing orders occur due to the interplay between the localized tendency arising from the strong Coulomb repulsion and the delocalization due to the mobilities of carriers. An interesting order tendency is the nematic order,<sup>1</sup> which breaks the four-fold rotational symmetry of the underlying crystal but retains the translational symmetry of the system. Recent neutron scattering<sup>2</sup> and Nernst effect<sup>3</sup> measurements of  $\text{YBa}_2\text{Cu}_3\text{O}_y$  provided strong evidences for the existence of nematic state in the underdoped cuprates. Moreover, a spectroscopic-imaging scanning tunneling microscope (STM) investigation on  $\text{Bi}_2\text{Sr}_2\text{CaCu}_2\text{O}_{8+\delta}$ <sup>4</sup> suggested an intra-unit-cell (IUC) electronic nematic state which breaks the  $90^\circ$  - rotational symmetry within every  $\text{CuO}_2$  unit cell.

Theoretical studies on the two-dimensional  $t$ - $J$ <sup>5-7</sup> and Hubbard<sup>8-12</sup> models have reported a spontaneous  $d$ FSD instability in the underdoped region: the Fermi surface (FS) expands along the  $k_x$  direction and shrinks along the  $k_y$  direction or vice versa. This order is considered to be generated by a forward scattering of electrons close to the FS near  $(0, \pi)$  and  $(\pi, 0)$ , which breaks the orientational symmetry but keeps the translational symmetry of the system. From the symmetry point of view such a state naturally leads to an electronic nematic order. However, theoretical studies on the nematic order have so far mainly focused on the one-band models or in the extreme limit of infinite interactions<sup>13</sup>. A recent mean field analysis of a more realistic model, i.e. the three-band Hubbard model<sup>14</sup>, showed that the Coulomb interaction between next nearest-neighbor (NNN) oxygen atoms  $V_{pp}$  plays a crucial role in the formation of the nematic order<sup>15</sup>, which demonstrates that the interaction within the unit cell on the  $\text{CuO}_2$  plan is needed to be taken into account in order to show

the delicate mechanism and to depict a clear picture of the nematic order in the cuprates.

To gain a further insight into the nematic order in the cuprates, we carry out a systematic variational Monte Carlo (VMC) study on  $d$ FSD within the three-band Hubbard model. Interestingly, we find that the electronic nematicity has already shown up at  $V_{pp} = 0$ , and becomes stronger with  $V_{pp}$  increasing. We also find that while both the copper on-site Coulomb interaction  $U_d$  and the charge-transfer energy  $\Delta_{ct}$  have a remarkable positive effect on  $d$ FSD, the NNN oxygen-oxygen hopping  $t_{pp}$  has a negative effect. Our results are qualitatively in agreement with the slave-boson mean field (SBMF) calculations<sup>5</sup> over a wide doping range, showing that  $d$ FSD has the strongest tendency around the van Hove filling<sup>8,9,12,16,17</sup> (namely half-filling in our calculations) in the absence of magnetism. Beyond that, we show that  $d$ FSD in the three-band model leads to an imbalance in the hole densities of the neighboring oxygen sites, providing a consistent theoretical explanation on the phenomena observed by STM in  $\text{Bi}_2\text{Sr}_2\text{CaCu}_2\text{O}_{8+\delta}$ <sup>4</sup>.

The paper is organized as follows: In Sec.II we define the three-band Hubbard model and outline the VMC scheme. Results from this numerical solution and comparisons with previous studies are presented in Sec.III. A conclusion is given in Sec.IV.

## II. MODEL HAMILTONIAN AND METHODS

By considering the energetics and hybridizations for copper  $3d_{x^2-y^2}$  orbital and oxygen  $2p_x$  ( $2p_y$ ) orbital, the kinetic part

of the three-band model reads,

$$H_0 = \varepsilon_d \sum_{i,\sigma} n_{i,\sigma}^d + \varepsilon_p \sum_{i,\sigma} \sum_{\nu} n_{i+\nu/2,\sigma}^p - t_{pd} \sum_{i,\sigma} \sum_{\nu} (d_{i,\sigma}^\dagger p_{i+\nu/2,\sigma} + h.c.) - t_{pp} \sum_{i,\sigma} \sum_{\langle \nu, \nu' \rangle} (p_{i+\nu/2,\sigma}^\dagger p_{i+\nu'/2,\sigma} + h.c.), \quad (1)$$

where  $d_{i,\sigma}^\dagger$  and  $p_{i+\nu/2,\sigma}^\dagger$  create a hole with spin  $\sigma$  at the  $i$ th copper site and the  $i + \nu/2$ th oxygen site, respectively, with  $\nu = a_x(a_y)$  being the unit vectors along the  $x$  and  $y$  directions.  $n_{i,\sigma}^d$  and  $n_{i+\nu/2,\sigma}^p$  are the corresponding number operators.  $t_{pd}$  and  $t_{pp}$  denote the copper-oxygen and oxygen-oxygen hopping integrals.  $\langle \nu, \nu' \rangle$  limits the sum over NNN oxygen-oxygen lattice sites. We set  $\varepsilon_d \equiv 0$  on the copper site and introduce the charge-transfer energy  $\Delta_{ct} = \varepsilon_p - \varepsilon_d$  to control the relative Cu/O hole densities.

The interaction part of the model is given by,

$$H' = U_d \sum_i n_{i\uparrow}^d n_{i\downarrow}^d + \frac{U_p}{2} \sum_{i,\nu} n_{i+\nu/2,\uparrow}^p n_{i+\nu/2,\downarrow}^p + V_{pd} \sum_{i,\nu} \sum_{\sigma,\sigma'} n_{i,\sigma}^d n_{i+\nu/2,\sigma'}^p + V_{pp} \sum_{i,\langle \nu, \nu' \rangle} \sum_{\sigma,\sigma'} n_{i+\nu/2,\sigma}^p n_{i+\nu'/2,\sigma'}^p, \quad (2)$$

here  $U_d$  and  $U_p$  are the on-site Coulomb interactions on the copper and oxygen sites, respectively.  $V_{pd}$  and  $V_{pp}$  are the Coulomb repulsions between nearest-neighbor (NN) copper-oxygen sites and NNN oxygen-oxygen sites, respectively. In the following, the parameters within  $\text{CuO}_2$  plane are measured in the unit of  $t_{pd}$ .

We use the following variational wave function:

$$|\psi\rangle = P_G \prod_{|k| \leq k_F, \sigma} \alpha_{k\sigma}^\dagger |0\rangle, \quad (3)$$

where  $P_G = P_d P_p P_{pd} P_{pp}$  is the projection operator, which contains four parts: 1.  $P_d = \prod_i (1 - (1 - g_d) n_{i\uparrow}^d n_{i\downarrow}^d)$  modifies the double occupancy on the Cu site; 2.  $P_p = \prod_{i,\nu} (1 - (1 - g_p) n_{i+\nu/2,\uparrow}^p n_{i+\nu/2,\downarrow}^p)$  modifies the double occupancy on the O site; 3.  $P_{pd} = \prod_{i,\nu} g_{pd} n_{i,\uparrow}^d n_{i+\nu/2,\uparrow}^p$  adjusts the charge occupancies on the NN copper-oxygen sites; 4.  $P_{pp} = \prod_{i,\langle \nu, \nu' \rangle} g_{pp} n_{i+\nu/2,\uparrow}^p n_{i+\nu'/2,\uparrow}^p$  adjusts the charge occupancies on the NNN oxygen-oxygen sites. Here  $g_d, g_p, g_{pd}$ , and  $g_{pp}$  stand for four variational parameters in the range from 0 to 1, which will be optimized during the Monte Carlo calculations.

In Eq. (3), the single-particle operator  $\alpha_{k\sigma}^\dagger$  is given by a linear combination of  $d_{k\sigma}^\dagger$ ,  $p_{xk\sigma}^\dagger$ , and  $p_{yk\sigma}^\dagger$ , which are the Fourier transformations of  $d$ - and  $p$ - hole operators:

$$d_{k,\sigma}^\dagger = \frac{1}{\sqrt{N}} \sum_i d_{i,\sigma}^\dagger e^{-ikr_i}, \quad (4)$$

$$p_{\nu k,\sigma}^\dagger = \frac{1}{\sqrt{N}} \sum_i p_{i+\nu/2,\sigma}^\dagger e^{-ikr_{i+\nu/2}}, \quad (5)$$

where  $N$  is the total number of unit cells. The coefficients in  $\alpha_{k\sigma}^\dagger$  are obtained through diagonalizing the following matrix,

$$H_{eff} = \begin{pmatrix} \Delta_{eff} & -4t_{pp} \cos \frac{k_x}{2} \cos \frac{k_y}{2} & -2t_{pd,x} \cos \frac{k_x}{2} \\ -4t_{pp} \cos \frac{k_x}{2} \cos \frac{k_y}{2} & \Delta_{eff} & -2t_{pd,y} \cos \frac{k_y}{2} \\ -2t_{pd,x} \cos \frac{k_x}{2} & -2t_{pd,y} \cos \frac{k_y}{2} & 0 \end{pmatrix}, \quad (6)$$

here  $\Delta_{eff}$  is a variational parameter acting as an effective charge-transfer energy. Introducing an asymmetry parameter  $\delta_{var}$  between the hopping integrals along  $x$  and  $y$  direction, we have

$$t_{pd,x} = t_{pd} - \delta_{var}, \quad (7)$$

$$t_{pd,y} = t_{pd} + \delta_{var}. \quad (8)$$

When  $\delta_{var}$  is finite, the shape of FS is deformed. We evaluated the expectation value of total energy for the variational wave-function by employing Monte Carlo method<sup>18-23</sup>. The four projection parameters  $g_d, g_p, g_{pd}$ , and  $g_{pp}$ , as well as the effective charge-transfer energy  $\Delta_{eff}$  and the asymmetry parameter  $\delta_{var}$ , are optimized to obtain the minimal energy. During the optimization, a quasi-Newton method combined with the fixed sampling method<sup>24,25</sup> is used. The calculations have been done for square lattices with periodic and antiperiodic boundary conditions along the  $x$  and  $y$  direction, respectively. These boundary conditions are used to avoid the degenerate states at the Fermi surface. Typically,  $10^7$  Monte Carlo steps are performed for each set of variational parameters. The resulting statistical errors are given in the relevant figures by error bars.

### III. NUMERICAL RESULTS AND DISCUSSIONS

In the present paper, we take the typical values of the copper oxide parameters. Setting the copper-oxygen hopping  $t_{pd} \equiv 1$ , we have  $U_d = 8.0$ ,  $U_p = 3.0$ ,  $V_{pd} = 1.0$ , and  $\Delta_{ct} = 3.0$ , according to the constrained density-functional calculations<sup>26</sup>.  $t_{pp}$  is expected to have a negative effect on  $d\text{FSD}$ , so we will firstly focus on the case of  $t_{pp}=0.0$  and the order dependence on  $t_{pp}$  will be examined alone later on. The results presented below are obtained for these typical parameters, except where explicitly noted otherwise.

Firstly, in Fig.1 (a), we present the doping dependence of the condensation energy per unit cell ( $E_{cond} = [E(\delta_{var}^{opt}) - E(0)]/N$ , with  $\delta_{var}^{opt}$  being the optimized asymmetry parameter) on the square lattices of the sizes of  $16 \times 16$ ,  $20 \times 20$ , and  $22 \times 22$ . One can observe that for all the three lattices, the absolute value of  $E_{cond}$  decreases continuously from half-filling and vanishes at  $n_h \sim 1.15$ . This behavior is consistent with the slave-boson mean-field (SBMF) analysis for the  $t - J$  model, indicating that the growing forward scattering with decreasing hole density has a positive contribution to the formation of the  $d\text{FSD}$  state. Fig.1 (b) shows the dependence of  $\delta_{var}^{opt}$  on the hole density. There is an obvious tendency that

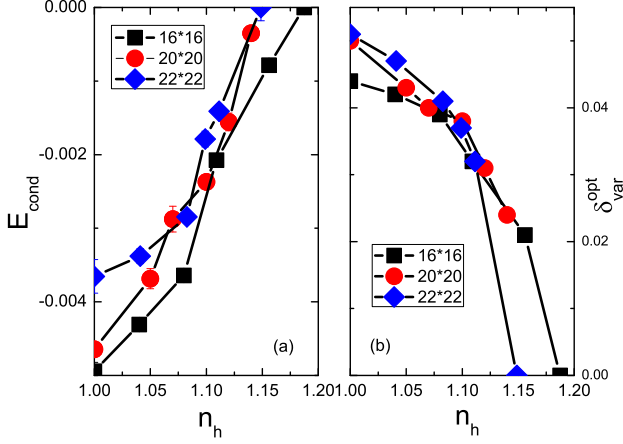


FIG. 1: (Color online) Condensation energy  $E_{\text{cond}}$  (a) and optimized value of  $\delta_{\text{var}}$  (b) as a function of hole density  $n_h$  on the 16×16, 20×20, and 22×22 lattices.

$\delta_{\text{var}}^{\text{opt}}$  decreases to zero at  $n_h \sim 1.15$  in the same way as the condensation energy, suggesting that  $d\text{FSD}$  only occurs in the underdoped region.

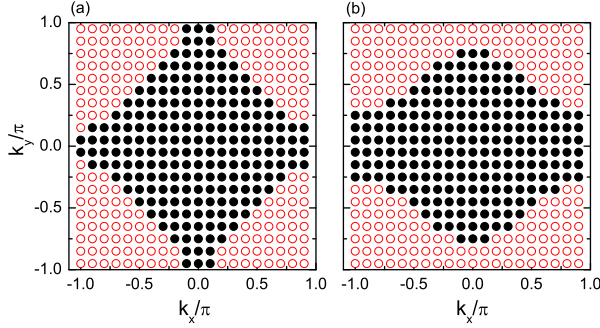


FIG. 2: (Color online) Fermi surfaces in the normal state ( $\delta_{\text{var}}=0.0$ ) (a) and the  $d\text{FSD}$  state ( $\delta_{\text{var}}=0.062$ ) (b) at the hole density  $n_h=1.05$ . Filled (empty) sites indicate the occupied (unoccupied)  $k$  points.

We present the isotropic ( $\delta_{\text{var}}=0.0$ ) and distorted ( $\delta_{\text{var}}=0.062$ ) FS's at  $n_h=1.05$  for a 20×20 square lattice in Fig.2. It is shown that the four fold rotational symmetry of FS is reduced to two fold in the distorted ground state. The FS expands along the  $k_x$  direction and shrinks along the  $k_y$  direction as the optimized  $\delta_{\text{var}}$  takes a positive value. We learn from Fig.2 that the finite size effect brings some difficulties in determining the optimal value of  $\delta_{\text{var}}$  in our calculations: when the FS is distorted by a nonzero  $\delta_{\text{var}}$ , the states near  $(0,\pi)$  or  $(\pi,0)$  undergo a discontinuous change from unoccupied to occupied or vice versa. This kind of discontinuity introduces an uncertainty of the optimal value of  $\delta_{\text{var}}$ , which is estimated about 0.01~0.02 for our studied systems.

From Fig.1, it can be seen that the  $d\text{FSD}$  state is stablest at half-filling. However, strong  $(\pi, \pi)$  scattering around half-filling may favor an antiferromagnetic (AFM) state, instead of the  $d\text{FSD}$  state. To clarify this issue, we carried out VMC cal-

culations for the projected AFM state at half-filling, and the corresponding condensation energy per unit cell is  $-0.2185$  and  $-0.2266$  on the 16×16 and 20×20 lattices, respectively. Two order lower of the condensation energy in the AFM state compared to the  $d\text{FSD}$  state demonstrates that magnetic ordering is actually the strongest instability close to half-filling. With the increase of doping concentration, the AFM order quickly disappears in doped cuprates, and the ground state could be well described by a wave function without long-range magnetic ordering, such as the one in Eq. (3).

Another long-range order that may compete with  $d\text{FSD}$  is the  $d$ -wave superconductivity, which is induced by AFM spin fluctuations. According to the VMC study of the one-band  $t$ - $J$  model<sup>7</sup>, the  $d\text{FSD}$  instability is overwhelmed by the  $d$ -wave superconductivity. However, in the case of the three-band Hubbard model, a VMC study<sup>27</sup> showed that the superconducting condensation energy is about  $10^{-3}$ , which is comparable to the energy gain in the  $d\text{FSD}$  state by our calculations. This indicates that the  $d\text{FSD}$  instability is as strong as the superconducting instability in the three-band Hubbard model. A further study is needed to clarify one remaining question, whether both  $d\text{FSD}$  and  $d$ -wave superconductivity can coexist in the multi-band model.

To understand the physical origin for the formation of  $d\text{FSD}$ , we present different energy changes  $\Delta E_\alpha = (E_\alpha(\delta_{\text{var}}) - E_\alpha(0))/N$  as a function of  $\delta_{\text{var}}$ , with  $\alpha$  representing different components of the Hamiltonian in Fig. 3. We observe that while  $\Delta E_{\text{kin}}$  and  $\Delta E_{U_p}$  take positive values as the system changes into an anisotropic state, the other three components  $\Delta E_{U_d}$ ,  $\Delta E_{V_{pd}}$ , and  $\Delta E_{\Delta_{ct}}$  take negative values in the studied parameter region, which lower the total energy of the system, and lead to a minimum at a certain value of  $\delta_{\text{var}}$ . This reveals that the  $d\text{FSD}$  state is the result of delicate competition between the localized tendency introduced by  $U_d$ ,  $V_{pd}$ ,  $\Delta_{ct}$  and the delocalization due to the kinetic term of carriers. One can notice that the dependence of different energy changes on  $\delta_{\text{var}}$  shows similar behavior both at half-filling ( $n_h = 1$ ) and at a finite hole doping density ( $n_h = 1.05$ ). This is rather different from the VMC study of the  $t$ - $J$  model at half-filling<sup>6</sup>, where the kinetic energy is exact zero and the  $J$  induced superexchange energy is found to increase with  $\delta_{\text{var}}$  increasing, resulting in the vanishing of condensation energy at half-filling.

To explore the parameter dependence of the  $d\text{FSD}$  state, we present the change of total energy  $\Delta E = [E(\delta_{\text{var}}) - E(0)]/N$  as a function of  $\delta_{\text{var}}$  for different sets of parameters at a fixed doping ( $n_h = 1.05$ ) in Figs. 4-6. From Fig.4, one sees that the on-site Coulomb interaction on the copper sites,  $U_d$ , has a remarkable positive effect on  $d\text{FSD}$ , manifested by a decrease of  $\Delta E$  with increasing  $U_d$  and a shift of minimum to larger  $\delta_{\text{var}}$ . This can be expected since  $U_d$  makes a dominant contribution to the forward scattering, which is considered to be the origin of  $d\text{FSD}$ . As seen in Fig. 5, a decrease of  $\Delta E$  with increasing  $V_{pd}$  or  $\Delta_{ct}$  indicates that both NN copper-oxygen repulsion and charge-transfer energy have a positive effect on the formation of  $d\text{FSD}$ . It is naturally to expect that when  $V_{pd}$  or  $\Delta_{ct}$  increases, more holes transfer from oxygen sites to copper sites, resulting in a stronger forward scattering of carriers by  $U_d$ .

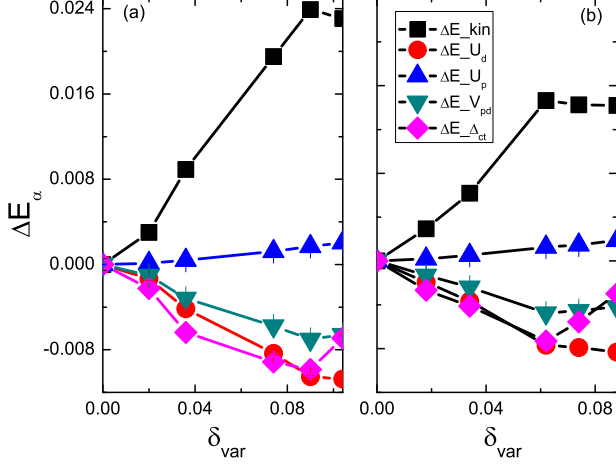


FIG. 3: (Color online) Different energy changes as a function of  $\delta_{\text{var}}$  on the  $20 \times 20$  lattice. (a)  $n_h=1$ , (b)  $n_h=1.05$ .

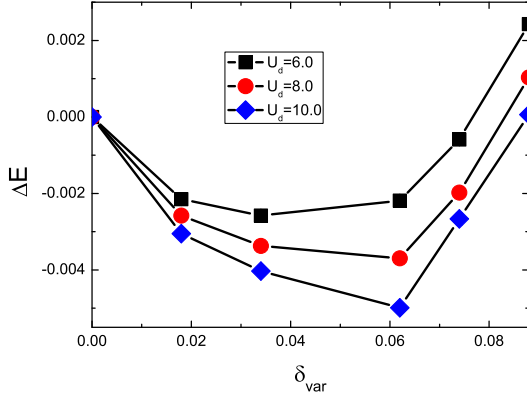


FIG. 4: (Color online) Total energy change as a function of  $\delta_{\text{var}}$  for different values of  $U_d$ . Lattice =  $20 \times 20$  and  $n_h=1.05$ .

Once  $t_{pp}$  turns on, it may enhance the delocalization of holes on the oxygen sites, and have a strong negative effect on  $d\text{FSD}$ . To examine if  $d\text{FSD}$  exists in the actual cuprates materials, we compare the change of total energy  $\Delta E$  for  $t_{pp} = 0.0$  and  $t_{pp} = 0.4$  in Fig. 6. It is readily seen that although the condensation energy at  $t_{pp}=0.4$  is much smaller than the case of  $t_{pp}=0.0$ , the  $d\text{FSD}$  state still survives.

The NNN oxygen-oxygen Coulomb repulsion  $V_{pp}$  is expected to have a positive effect on  $d\text{FSD}$ , since it favors an inhomogeneity in the hole densities of the NNN oxygen sites. In the previous work by Fischer et al.<sup>15</sup>, a mean field analysis based on the three-band model showed that the minimum value of  $V_{pp}$  that needed for a system to enter a nematic phase is about 1.2, which is much higher than the realistic value. Here, in Fig.6, we show that the electronic nematicity has already shown up at  $V_{pp}=0$ , and becomes stronger if we introduce  $V_{pp}=0.5$ . Our results demonstrate that a spontaneous  $d\text{FSD}$  can occur in actual cuprates materials.

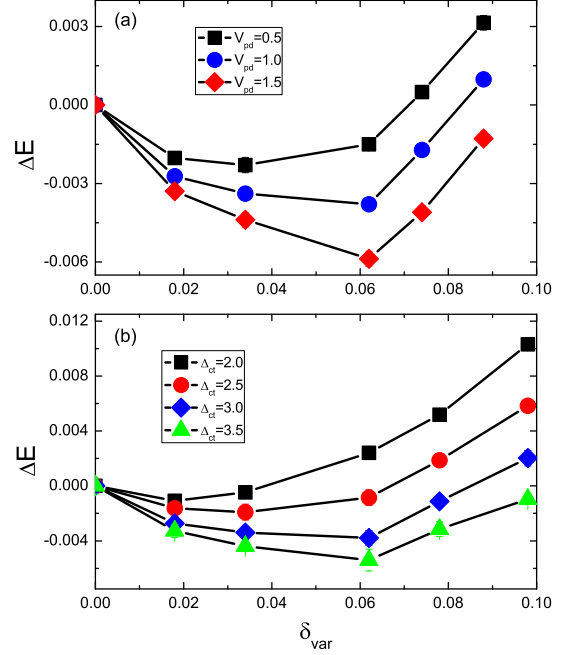


FIG. 5: (Color online) Dependence of total energy change on  $\delta_{\text{var}}$  for different values of  $V_{pd}$  (a) and  $\Delta_{ct}$  (b) on the  $20 \times 20$  lattice and  $n_h=1.05$ .

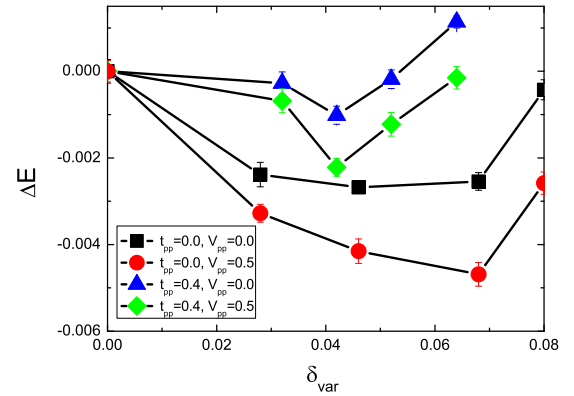


FIG. 6: (Color online) Total energy change as a function of  $\delta_{\text{var}}$  for different values of  $t_{pp}$  and  $V_{pp}$ . Lattice =  $20 \times 20$  and  $n_h=1.07$ .

As mentioned before, an STM investigation on  $\text{Bi}_2\text{Sr}_2\text{CaCu}_2\text{O}_{8+\delta}$  showed that there exists a significant density difference in the two oxygen sites within each unit cell. In Fig.7, we present the hole densities on the copper and oxygen sites for the  $20 \times 20$  lattice, at  $n_h=1.05$ . The inhomogeneous distribution of hole densities in the  $p_x$  and  $p_y$  oxygen orbitals indicates that  $d\text{FSD}$  in the three-band model naturally results in an IUC nematicity, which is in good agreement with the results of the STM investigation. In

the investigation of high- $T_c$  cuprates, nematic order is usually considered to be the result of melted stripes<sup>2,3</sup>, namely, arising from proliferation of dislocations, the topological defects in the striped state<sup>28</sup>. However, although a striped state may have a close relation to the nematic order, the  $d$ FSD instability can also lead directly to an electronic nematic state, as shown in Fig.7.

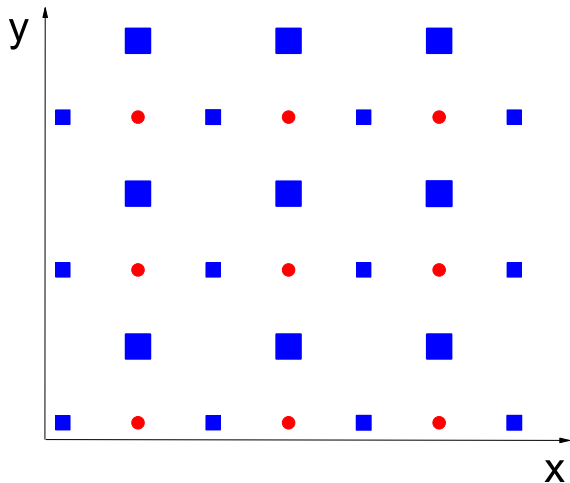


FIG. 7: (Color online) Distribution of hole densities on the copper and oxygen sites. The results are obtained for the  $20 \times 20$  lattice at  $n_h=1.05$ . The length of blue squares represents the hole density at  $O_x$  and  $O_y$  sites, red circles indicate the locations of Cu sites.

#### IV. CONCLUSION

In summary, our VMC study on the three-band Hubbard model show that there exists a  $d$ FSD instability in the realistic

parameter region of cuprates, which is weakened with increasing the hole doping density and vanishes at  $n_h \sim 1.15$ . The resulting imbalance of hole densities on the NNN oxygen sites confirms that  $d$ FSD is a possible origin for the IUC nematic phenomena, which was firstly proposed by Lawler *et al.*<sup>4</sup>. Our results show a qualitative agreement with the experimental results<sup>2-4</sup> and are consistent with the SBMF calculations for the  $t$ - $J$  model<sup>5</sup>. An analysis of the order dependence of  $d$ FSD on various parameters within the three-band model showed that  $U_d$ ,  $V_{pd}$ , and  $\Delta_{ct}$  have a remarkable positive effect on  $d$ FSD. They contribute to the formation of  $d$ FSD in such a way that the forward scattering is enhanced either by increasing  $U_d$  or through transferring holes from oxygen to copper sites as  $V_{pd}$  ( $\Delta_{ct}$ ) becomes larger. We found that  $d$ FSD survives when a finite oxygen-oxygen hopping integrals  $t_{pp}$  is introduced, and if a finite  $V_{pp}$  interaction exists, the  $d$ FSD state will be stabler.

Recently, the experimental evidence for electronic anisotropy in iron-based superconductors has been accumulated<sup>29-34</sup>. The situation in iron-based superconductors is much more complicate since the lattice, spin, and orbital degrees of freedom all manifest themselves in the nematic state<sup>35</sup>. We consider that our VMC study for the cuprates can be generalized to iron-based superconductors and may be helpful for clarifying the nematicity in these systems.

#### Acknowledgments

This work was supported by the NSFC of China under Grant No. 11074257 and 11274310. Z.B.H. was supported by NSFC under Grant Nos. 10974047 and 11174072, and by SRFDP under Grant No.20104208110001. Numerical calculations were performed in Center for Computational Science of CASHIPS.

\* Electronic address: huangzb@hubu.edu.cn

† Electronic address: zou@theory.issp.ac.cn

<sup>1</sup> S. A. Kivelson, E. Fradkin, and V. J. Emery, Nature (London) 393, 550 (1998)

<sup>2</sup> V. Hinkov, D. Haug, B. Fauque, P. Bourges, Y. Sidis, A. Ivanov, C. Bernhard, C. T. Lin, and B. Keimer, Science 319, 597 (2008).

<sup>3</sup> R. Daou, J. Chang, D. LeBoeuf, O. Cyr-Choiniere, F. Laliberte, N. Doiron-Leyraud, B. J. Ramshaw, R. Liang, D. A. Bonn, W. N. Hardy, and L. Taillefer, Nature (London) 463, 519 (2010).

<sup>4</sup> M. Lawler, K. Fujita, L. Jhinwhan, A. R. Schmidt, Y. Kohsaka, Chung Koo Kim, H. Eisaki, S. Uchida, J. C. Davis, J. P. Sethna, and Eun-Ah Kim, Nature (London) 466, 347 (2010).

<sup>5</sup> H. Yamase and H. Kohno, J. Phys. Soc. Jpn. 69, 2151 (2000).

<sup>6</sup> A. Miyazawa and H. Yamase, Phys. Rev. B 73, 174513 (2006).

<sup>7</sup> B. Edegger, V. N. Muthukumar, and C. Gros, Phys. Rev. B 74, 165109 (2006).

<sup>8</sup> C. J. Halboth and W. Metzner, Phys. Rev. Lett. 85, 5162 (2000).

<sup>9</sup> B. Valenzuela and M. A. H. Vozmediano, Phys. Rev. B 63, 153103 (2001).

<sup>10</sup> V. Hankevych, I. Grote, and F. Wegner, Phys. Rev. B 66, 094516 (2002).

<sup>11</sup> A. P. Kampf and A. A. Katanin, Phys. Rev. B 67, 125104 (2003).

<sup>12</sup> A. Neumayr and W. Metzner, Phys. Rev. B 67, 035112 (2003)

<sup>13</sup> S. A. Kivelson, E. Fradkin, and T. H. Geballe, Phys. Rev. B 69, 144505 (2004).

<sup>14</sup> V. J. Emery, Phys. Rev. Lett. 58, 2794 (1987).

<sup>15</sup> M. H. Fischer and E.-A. Kim, Phys. Rev. B 84, 144502 (2011).

<sup>16</sup> H. Yamase, V. Oganessian, and W. Metzner, Phys. Rev. B 72, 035114 (2005).

<sup>17</sup> H. Yamase and W. Metzner, Phys. Rev. B 75, 155117 (2007).

<sup>18</sup> C. Gros, Phys. Rev. B 38, 931 (1988).

<sup>19</sup> H. Yokoyama and H. Shiba, J. Phys. Soc. Jpn. 57, 2482 (1988)

<sup>20</sup> H. Yokoyama and M. Ogata, *ibid.* 65, 3615 (1996).

<sup>21</sup> K. Yamaji, T. Yanagisawa, T. Nakanishi, and S. Koike, J. Phys. Soc. Jpn. 304, 225 (1998).

<sup>22</sup> F. Becca, M. Capone, and S. Sorella, Phys. Rev. B 62, 12700 (2000).

<sup>23</sup> A. Paramekanti, M. Randeria, and N. Trivedi, Phys. Rev. Lett. 87,

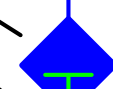
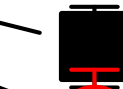
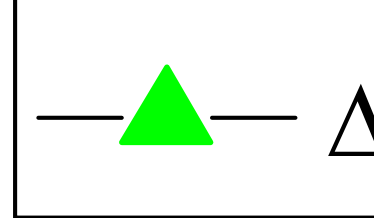
- 217002 (2001); Phys. Rev. B 70, 054504 (2004).
- <sup>24</sup> D. Ceperley, G. V. Chester, and K. H. Kalos, Phys. Rev. B 16, 3081 (1977).
- <sup>25</sup> C. J. Umrigar, K. G. Wilson, and J. W. Wilkins, Phys. Rev. Lett. 60, 1719 (1988).
- <sup>26</sup> M. S. Hybertsen, M. Schlüter, and N. E. Christensen, Phys. Rev. B, 39, 9028 (1989).
- <sup>27</sup> T. Yanagisawa, S. Koike, and K. Yamaji, Phys. Rev. B 64, 184509 (2001).
- <sup>28</sup> E. Fradkin, S. A. Kivelson, M. J. Lawler, J. P. Eisenstein, and A. P. Mackenzie, Annu. Rev. Condens. Matter Phys. 1, 153 (2010).
- <sup>29</sup> T.-M. Chuang, M. P. Allan, J. Lee, Y. Xie, N. Ni, S. L. Budko, G. S. Boebinger, P. C. Canfield, and J. C. Davis, Science 327, 181 (2010).
- <sup>30</sup> J.-H. Chu, J. G. Analytis, K. De Greve, P. L. McMahon, Z. Islam, Y. Yamamoto, and I. R. Fisher, Science 329, 824 (2010).
- <sup>31</sup> R. M. Fernandes, L. H. VanBebber, S. Bhattacharya, P. Chandra, V. Keppens, D. Mandrus, M. A. McGuire, B. C. Sales, A. S. Sefat, and J. Schmalian, Phys. Rev. Lett. 105, 157003 (2010).
- <sup>32</sup> I. R. Fisher, L. Degiorgi, and Z. X. Shen, Rep. Prog. Phys. 74, 124506 (2011).
- <sup>33</sup> J. J. Ying, X. F. Wang, T. Wu, Z. J. Xiang, R. H. Liu, Y. J. Yan, A. F. Wang, M. Zhang, G. J. Ye, P. Cheng, et al., Phys. Rev. Lett. 107, 067001 (2011).
- <sup>34</sup> M. Yi, D. H. Lu, J.-H. Chu, J. G. Analytis, A. P. Sorini, A. F. Kemper, B. Moritz, S.-K. Mo, R. G. Moore, M. Hashimoto, W.-S. Lee, Z. Hussain, T. P. Devereaux, I. R. Fisher, and Z.-X. Shen, PNAS 108, 6878 (2011).
- <sup>35</sup> J Hu, C Xu, arXiv:1112.2713, (2011)

$E_{\text{cond}}$

0.000

-0.005

0.00



$E_{\text{cond}}$

-0.002

-0.004

1.00

1.04

